JOURNAL OF GEOPHYSICAL RESEARCH, VOL. 102, NO. D23, PAGES 28,185–28,193, DECEMBER 20, 1997

Polar stratospheric clouds due to vapor enhancement: HALOE observations of the Antarctic vortex in 1993

M. E. Hervig[1], K. S. Carslaw[2], T. Peter[2], T. Deshler[1], L. L. Gordley[3], G. Redaelli[4], U. Biermann[2], and J. M. Russell III[5]

Abstract. Aerosol measurements from the Halogen Occultation Experiment (HALOE) during the Antarctic spring of 1993 are compared with calculations of the volume of different types of polar stratospheric clouds (PSCs) at equilibrium. The observed volumes increased by a factor of ~30 coincident with water vapor enhancements of ~3 ppmv, suggesting that the enhancement of water vapor was important in determining PSC growth. The enhanced water vapor was coincident with increased methane mixing ratios, and trajectory analysis suggests that the vapor enhancements were consistent with transport from lower latitudes. The nitric acid distribution was not measured and is treated either as constant or as positively correlated with the observed water. Comparing the observed volumes with model calculations assuming constant nitric acid suggests that the PSCs were composed of liquid ternary H_2SO_4–H_2O–HNO_3 aerosols (LTA) rather than solid nitric acid trihydrate (NAT). However, if the water vapor intrusions were accompanied by enhanced nitric acid, the observations closely match predictions for solid NAT, and those for LTA. These comparisons highlight the importance of the vapor distributions for modeling PSC growth and suggest that vapor resupply is important for late spring PSC growth. This work also highlights some inherent limitations of large field of view limb–viewing instruments for the observation of PSCs.

1. Introduction

Stratospheric temperatures during the polar winter and spring are often sufficiently low to allow the formation and growth of particles that can attain volumes 5–100 times greater than the background sulfuric acid–water aerosol, to form polar stratospheric clouds (PSCs). The current understanding of particles within PSCs suggests various possible compositions and phases [*Koop et al.*, 1997]. The most likely forms are liquid ternary H_2SO_4–H_2O–HNO_3 aerosols (LTA), solid nitric acid trihydrate (NAT), and water ice. Liquid H_2SO_4–H_2O aerosols can grow by the uptake of nitric acid and water vapors at temperatures below ~196 K [*Molina et al.*, 1993; *Carslaw et al.*, 1994; *Tabazadeh et al.*, 1994; *Carslaw et al.*, 1997] to form LTA. *Molina et al.* [1993] have suggested that solid NAT particles nucleate from the LTA droplets when supersaturation with respect to crystallization of NAT occurs. *Carslaw et al.* [1994] and later *Koop et al.* [1995, 1997] showed that the LTA probably remain liquid to temperatures at least as low as the ice frost point. The mechanism for nucleation of NAT remains a subject of debate [e.g., *Tolbert*, 1996]. For cooling below the water frost point, growth as water ice becomes the dominant process, regardless of the preexisting particle phase and composition.

PSC observations in the Arctic and Antarctic are consistent with the presence of both solid and liquid particles at different times. For example, analysis of in situ particle volume measurements made in the Arctic [*Dye et al.*, 1992] revealed that some PSCs were very likely composed of LTA droplets to the ice frost point (about 189 K) [*Carslaw et al.*, 1994; *Drdla et al.*, 1994; *Tabazadeh et al.*, 1994]. Other measurements, however, have been explained in terms of hydrates of nitric acid [*Dye et al.*, 1992; *Adriani et al.*, 1995; *Peter*, 1997] or solid solutions [*Tabazadeh and Toon*, 1996].

In this work, aerosol and water vapor measurements from the Halogen Occultation Experiment (HALOE) (version 18) during the austral spring of 1993 are compared with the calculated volumes for LTA, solid NAT, and ice. The calculations show that significant growth of either liquid or solid particles requires not only low temperatures but also mixing ratios of H_2O and HNO_3 that are higher than generally available in the spring Antarctic vortex.

2. HALOE Measurements

The HALOE instrument uses the principle of satellite solar occultation and the instrumental techniques of gas filter radiometry and broadband radiometry to measure profiles of solar attenuation by the atmosphere's limb as the Sun rises or sets relative to the spacecraft. Measurements in eight spectral bands (from 2.45 to 10.01 μm) are used to retrieve the profiles of HF, HCl, CH_4, NO, NO_2, H_2O, and O_3 mixing ratios, temperature, and aerosol extinction at 2.45, 3.40, 3.46, and 5.26 μm wavelengths. HALOE measurements cover two longitude sweeps each day (15 profiles each): one at the latitude of sunsets and one at the latitude of sunrises. Each HALOE sunrise (or sunset) measurement is separated by 1.6 hours and 24° longitude (which is 911 km at 70°S). HALOE sampling covers the Antarctic spring from roughly September 20 to October 20 reaching latitudes near 78°S.

The HALOE sample volume dimensions are determined by the instantaneous field of view (FOV) and the geometry of the atmospheric limb path. The vertical resolution of the measurements is ~2 km for retrievals of aerosol, NO_2, H_2O, and O_3, and ~4 km

[1]Department of Atmospheric Science, University of Wyoming, Laramie.
[2]Max–Planck–Institut für Chemie, Mainz, Germany.
[3]GATS Incorporated, Hampton, Virginia.
[4]Dipartimento di Fisica, University degli Studi, L'Aquila, Italy.
[5]Hampton University, Hampton, Virginia.

Paper number 97JD02464.
0148–0227/97/97JD–02464$09.00

for retrievals of HF, HCl, CH_4, and NO. The FOV length (along the limb) is determined mainly by the vertical resolution, and the width (across the limb) is determined mainly by the angle between the orbit plane and the satellite–Sun vector. The HALOE across–limb resolution (between 6 and 50 km) is close to the FOV width, and the along–limb dimension (320 km) is the limiting factor for observations of small–scale features. A complete description of the experiment is given by *Russell et al.* [1993a]. Of particular importance to this work are the HALOE retrievals of water vapor and aerosol extinction.

2.1 Aerosols

This work uses profiles of aerosol extinction retrieved from gas filter measurements in the 5.26 μm NO band [*Hervig et al.*, 1995]. A validation of the aerosol measurements by *Hervig et al.* [1996a] reports uncertainties of the order of ±15% for measurements in the middle and lower stratosphere. Growth of aerosol particles is most easily quantified in terms of the volume density (particle volume per unit volume of air). A theoretical relationship between volume density and extinction has been calculated from Mie theory based on a large number of aerosol size distributions measured using balloon–borne optical particle counters (OPCs). Thus the volume–extinction relationship is determined independently of HALOE and is used to convert HALOE extinctions to volumes. This work uses profiles measured in sulfate aerosols over Laramie, Wyoming (41°N), covering the complete cycle of the Mount Pinatubo volcanic aerosol cloud, and profiles measured in sulfate aerosols and PSCs over McMurdo Station, Antarctica (78°S) [see, for example, *Hofmann and Deshler*, 1991; *Deshler et al.*, 1994].

To determine the relationship for sulfate aerosols we have used 50 size distribution profiles measured over Laramie between August 1991 and March 1995. The balloonborne sampling did not include water vapor, and a constant 5 ppmv was assumed to compute the sulfate aerosol composition [*Steele and Hamill*, 1981]. The refractive index versus composition was determined according to *Palmer and Williams* [1975]. The results show a compact relationship between the extinctions and volumes (Figure 1) which were fit according to a power law relationship: $V = 1678.8\ \beta^{0.937}$, where β is the 5.26 μm extinction coefficient (km^{-1}) and V is the volume density ($\mu m^3\ cm^{-3}$). The relationship between extinction and volume is almost linear ($V \propto \beta^{0.937}$), as expected for a strongly absorbing medium.

Since the size distributions and refractive indices of PSC particles are different from those of sulfate aerosols, the volume–extinction relationship given above is expected to change for measurements in PSCs. The effect of inferring the volume in PSCs was investigated using size distributions measured in PSCs using OPCs over McMurdo Station during each Austral spring from 1990 to 1995. Using these size distributions, we assigned the refractive indices for either NAT [*Toon et al.*, 1994] or for ternary solutions to recalculate the volume–extinction relationships. The balloonborne sampling did not include water or nitric acid vapors, and constant mixing ratios were assumed (2 ppmv H_2O and 5 ppmv HNO_3) to determine the equilibrium temperature of NAT (T_{NAT}) [*Hanson and Mauersberger*, 1988] and the equilibrium composition of LTA [*Carslaw et al.*, 1995]. The calculations assuming NAT used all aerosol observations where the temperature was below T_{NAT} with the NAT refractive indices reported by *Toon et al.* [1994]. Thus, the relationship between 5.26 μm extinction and volume density was derived for NAT: $V = 1570.4\ \beta^{0.991}$, with units as above.

Refractive indices for ternary solutions have not yet been measured in the infrared region. To obtain them from existing

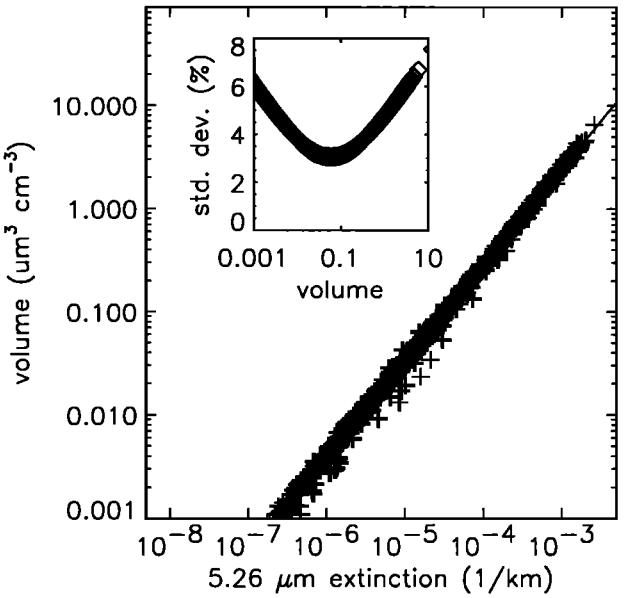

Figure 1. Calculated aerosol volume as a function of calculated 5.26 μm extinction using 50 size distribution profiles measured over Laramie, Wyoming, in sulfate aerosols. A fit to the 960 data points is shown (solid line), and the inset shows the standard deviation of the fit in volume.

indices for binary H_2O–H_2SO_4 [*Palmer and Williams*, 1975] and H_2O–HNO_3 [*Boone et al.*, 1980] solutions, we have used the Lorentz–Lorenz (L–L) mixing rule, which describes the refractivity for a mixture of different components. *Luo et al.* [1997] have shown that this technique can be applied successfully to typical stratospheric LTA compositions for wavelengths up to 2 μm. However, the strong absorption features of the ternary H_2SO_4–H_2O–HNO_3 system in the middle infrared region determine that application of the L–L rule is not straightforward. The L–L mixing rule assumes first, that the refractivity of a mixture can be obtained directly from a linear combination of the refractivities of the individual components, and second, that the refractivity is a function of the solution density, thereby allowing extrapolation to lower temperatures in terms of changes in the density alone. These assumptions certainly apply to the real part of the refractive index, as shown by *Luo et al.* [1997], but the imaginary component is seldom a linear combination of the component indices due to interactions between the absorbing molecules. In addition, these molecular interactions can change with decreasing temperature, and, in stratospherically relevant acids, the absorption features are also dependent on the dissociation constants of the acids, which change with aerosol composition and temperature.

Recent Fourier transform infrared (FTIR) thin film experiments [U. Biermann, dissertation in preparation, 1997] show that for the H_2SO_4–H_2O–HNO_3 system the L–L rule can be applied at least at certain wavelengths in the middle infrared. Specifically, the L–L rule can be applied in the 6.25 to 20 μm region (the sulfate and nitrate absorption regions of the ternary mixtures) and also with good reliability at 5.26 μm. The physical basis for this finding is that the absorption features are dependent on the overall acidity of the mixture and not on the precise composition. Extrapolation of the refractive index to lower temperatures according to the change in solution density is also more difficult to apply in the middle infrared, particularly since the H_2O–H_2SO_4 absorption spectra are strongly temperature dependent. However, at 5.26 μm the

absorption is small, thus allowing a reliable extrapolation to be made. We therefore use the 5.26 μm channel for our analysis, rather than the 3.46 μm channel. The relationships for LTA were determined from data where the calculated equilibrium nitric acid content of the droplets was greater than 10 wt % (typically temperatures less than about 194 K), with the appropriate (calculated) LTA index. Thus the relationship between 5.26 μm extinction and volume density was derived for LTA: $V=1940.9\beta^{0.965}$, with units as above.

The inferred PSC volumes calculated assuming either NAT or LTA are estimated to be within ±30% of those calculated by assuming sulfate aerosol. Instead of attempting to identify the correct refractive index, in the results below, extinctions were converted to volumes using the sulfate relationship with the nominal uncertainty of ±15–20% in volume increased to ±50%, to account for additional uncertainties in the volume determination. By doing so, we do not make an a priori assumption about the phase or composition of the particles, which would bias the results. As we show below, such an approach is necessary for cases where the PSC type cannot be determined unambiguously. Test calculations using either NAT or LTA indices reveal our assumption of ±50% uncertainty to be a true upper limit.

Aerosol measurements in PSCs probably contain signal from both cloud and background aerosol existing simultaneously in the sample volume. However, extinctions add linearly and PSC attenuation is typically a factor of 30 or more greater than for background aerosol, so the total extinction is essentially due to the PSC alone when both targets fill the field of view (FOV). A more important concern, however, is that the PSCs could have spatial dimensions that are smaller than the HALOE sample volume. Since the retrieved extinction (cross section per unit volume) is spatially smoothed over the FOV, degradation of the actual PSC extinction can occur when the cloud is nonuniform in the sample volume. We return to this issue later.

2.2. Water Vapor

Profiles of water vapor mixing ratio are retrieved from broadband radiometer measurements in the 6.62 μm H_2O band. These measurements are contaminated by aerosol absorption and are corrected using aerosol information retrieved independently at 5.26 μm wavelength. A major concern for the water vapor measurements in PSCs is the extrapolation of extinction from 5.26 μm to the water band–pass wavelength. The aerosol correction assumes sulfate aerosol size distributions and refractive indices but does not consider PSCs [*Hervig et al.*, 1995]. Test calculations using measured PSC size distributions and NAT refractive indices suggest that using the sulfate extrapolations in PSC contamination introduces errors of less than ±20% in the water vapor retrievals. A validation of the HALOE H_2O measurements by *Harries et al.* [1996] reports uncertainties of ±10% in the lower stratosphere, and increased uncertainties are considered below to account for the additional errors for retrievals in PSCs.

2.3. Temperature

HALOE transmission measurements in the 2.80 μm CO_2 band are used to retrieve profiles of temperature and pressure at altitudes above 35 km [*Hervig et al.*, 1996b]. For each HALOE measurement below 35 km altitude, a temperature profile is taken from the U.K. Meteorological Office (UKMO) record by interpolating the UKMO data to the HALOE measurement location and time. *Manney et al.* [1996] have shown that for the southern hemisphere under cold conditions (T < 200 K), the UKMO temperatures are generally unbiased with respect to radiosonde temperature observations and that the UKMO–radiosonde RMS temperature differences are less than 2 K.

3. HALOE Observations and Meteorological Situation

The HALOE aerosol, water vapor, and CH_4 measurements and the UKMO temperatures for the 1993 Antarctic spring are shown as orthographic projections on the 390 K potential temperature (θ) surface (Plate 1). The HALOE measurement latitude progressed from 50°S on October 4 to 75°S on October 9, giving a quasi–synoptic picture of the Antarctic region (since the measurements for different locations are at different times, such maps cannot be considered as truly synoptic). Each polygon in Plate 1 represents the true orientation and length of the HALOE FOV. The data are not contoured, as is typically done, since this would artificially introduce sub–FOV–scale gradients. The polygon representation highlights the problems associated with observations of non–FOV–filling features, which we return to later. PSCs are evident over the eastern shore of the Weddell Sea (which is at longitudes from roughly 300° to 0°) as enhanced aerosol extinction associated with low temperatures. The PSCs were present in measurements on October 7, 8, and 9 (at 71°S, 74°S, and 75°S, respectively) at potential temperatures from roughly 370 to 410 K (~120–80 mbar).

The potential vorticity (PV) field on the 390 K θ surface shows the boundary of the circumpolar vortex between 60°S and 65°S, as evidenced by the strong meridional gradient in PV (Plate 2). Low water vapor within the vortex boundary (Plate 1) is consistent with water vapor loss to PSC growth and sedimentation over the preceding winter and spring. The methane measurements (Plate 1) show reduced mixing ratios within the vortex boundary, which is consistent with large scale diabatic descent from higher altitudes within the vortex [*Russell et al.*, 1993b; *Rosenfield et al.*, 1994]. Over the eastern Weddell Sea and south of 65°S, however, the H_2O and CH_4 mixing ratios show a transition to values representative of lower latitudes. The observed water vapor enhancements of ~3 ppmv give an enhanced/ unenhanced ratio between 2 and 3. This ratio is consistent with in situ H_2O observations made inside and outside of the chemically perturbed region in the Antarctic stratosphere during the spring of 1987 [*Fahey et al.*, 1989]. Because methane is a conserved tracer, it can be used to indicate the origin of air [e.g., *Hartmann and Heidt*, 1989; *Murphy et al.*, 1989]. In this case, the enhanced CH_4 (and H_2O) mixing ratios over the Weddell Sea are consistent with transport from lower latitudes. Back–trajectory calculations using the National Center for Environmental Protection (NCEP) analysis were used to confirm this. Plate 3 shows the results of 670 ten–day isentropic back–trajectories ending in the region of interest on October 8. The colors indicate the latitudes (Plate 3a) and PV (Plate 3b) of the air parcels 10 days earlier. The locations and associated PV of the air parcels 10 days earlier is shown in Plate 3c. It is clear that the air in this region originated from lower latitudes where CH_4 and H_2O mixing ratios were generally higher (see the CH_4 and H_2O distributions in Plate 1). However, the PV of the air 10 days earlier was between -1.5×10^{-6} and -1.9×10^{-6}, indicating that the air originated from within, rather than from outside, the vortex. The enhanced mixing ratios of CH_4 and H_2O therefore appear to have been caused by mixing of vortex–edge air farther into the vortex, rather than by cross–vortex edge transport.

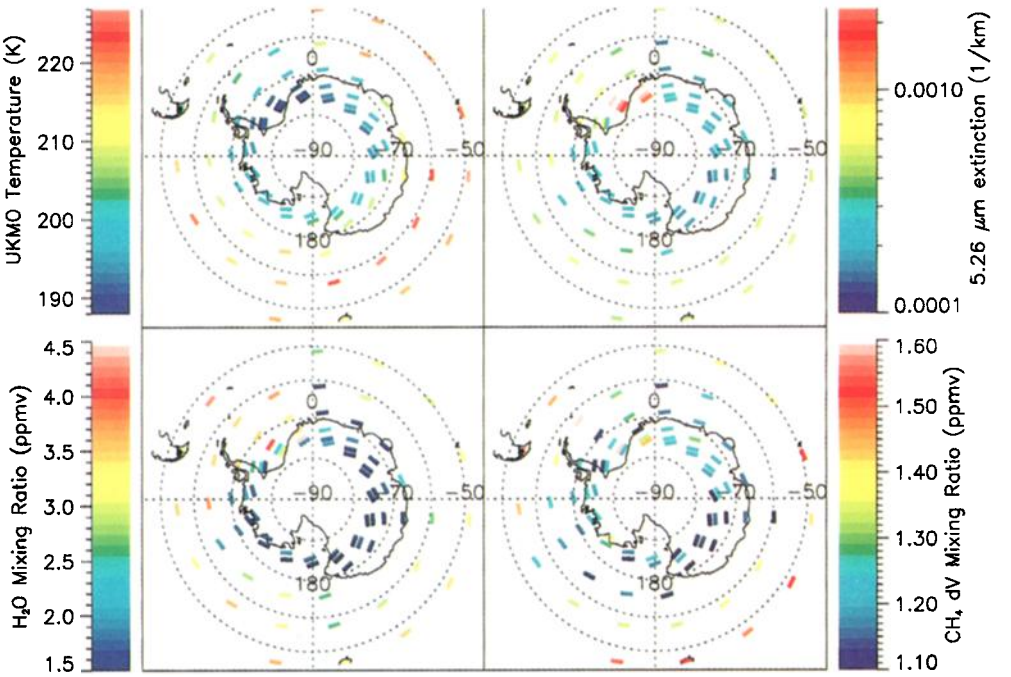

Plate 1. Orthographic projections from 50°S to 90°S on the 390 K potential temperature surface of temperature, 5.26 μm aerosol extinction, water vapor mixing ratio, and methane mixing ratio. The data are HALOE sunsets from October 4 (50°S) to October 9 (75°S), 1993. Each polygon represents the true orientation and length (along the limb) of the HALOE sample volume. The actual sample volume width (across the limb) was increased from ~50 to ~100 km for visual clarity.

4. Comparisons of Measured and Modeled PSC Volume

The measured volume densities are compared with the calculated volumes of different types of PSCs at equilibrium. Since only equilibrium states are considered, we do not require the specific temperature history of each air parcel, and it is therefore reasonable to include all PSC observations from this period (October 7–9) for these comparisons. In Figures 2 and 5, the measured and calculated volumes are shown versus temperature. However, it should be noted that this representation does not mean that each point is related to the others by a physical process

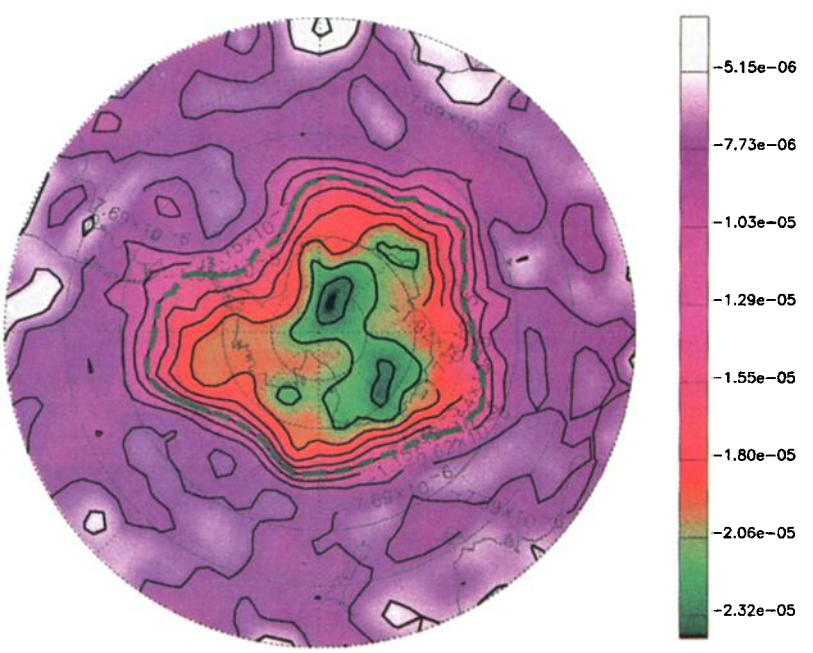

Plate 2. Potential vorticity (K m^2 kg^{-1} s^{-1}) on the 390 K θ surface for October 7, 1993. The bold green dashed line shows the vortex boundary. The data are from the National Center for Environmental Protection (NCEP, formerly NMC) analysis.

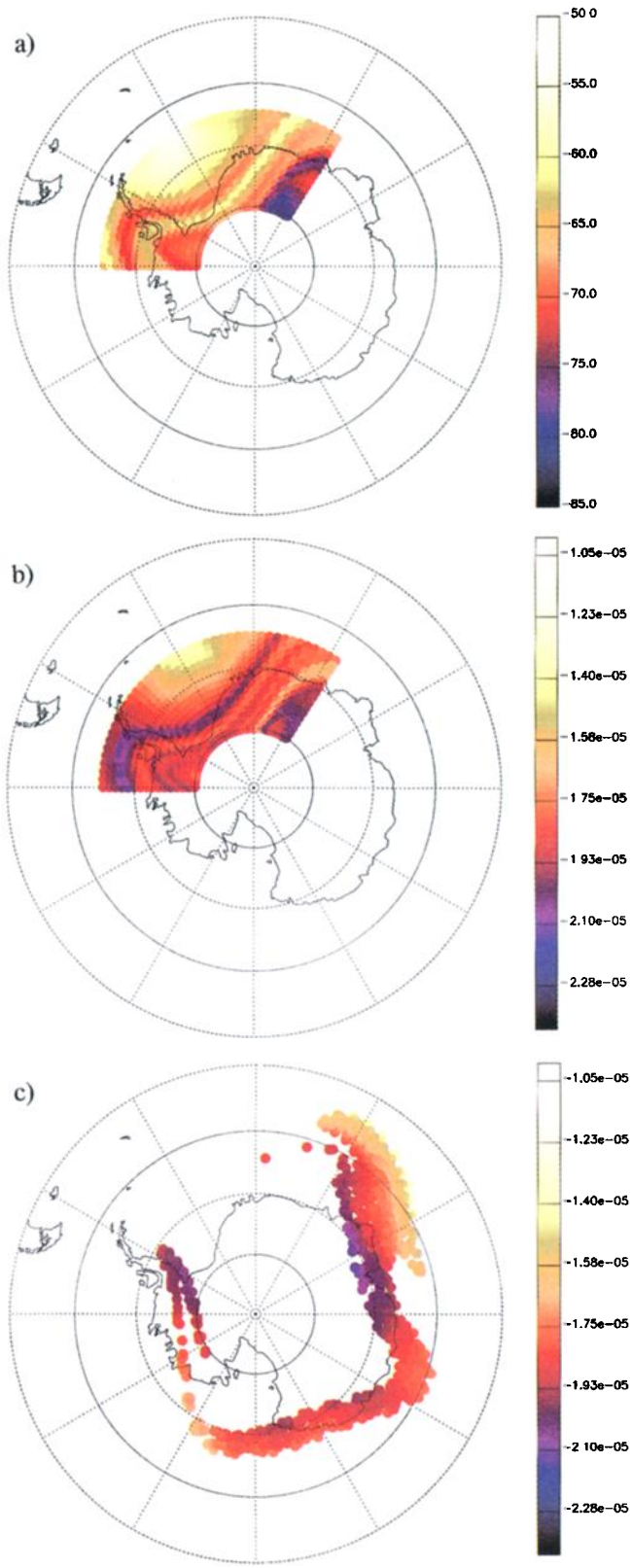

Plate 3. Results of 670 ten–day isentropic back–trajectories ending in the PSC region on October 8, on the 390 K θ surface. The colors indicate (a) the latitude of each air parcel 10 days earlier, and (b) the potential vorticity (PV) (K m^2 kg^{-1} s^{-1}) 10 days earlier. (c) The location of these air parcels 10 days earlier, with colors indicating the associated PV.

operating on a single aerosol sample, since each point is independent. HALOE aerosol volume and gas mixing ratio measurements on October 7–9 were interpolated in θ to the 390 K surface, and the observed water vapor mixing ratios were interpolated linearly in temperature between the observations for model input.

Saturation with respect to ice was predicted where the observed H_2O mixing ratios increased to about 4.5 ppmv at temperatures near 189 K (Figure 2a). At these temperatures the calculated equilibrium ice volumes were from ~50 to 100 μm^3 cm^{-3}, which is an order of magnitude greater than the observed volumes (Figure 2b). The amount of H_2O required to reach the ice point (T_{ice}) is shown in Figure 2a. If the observed H_2O mixing ratios were systematically ~25% too low, then all observations below 189 K would be at or below T_{ice}. On the other hand, if the observed H_2O mixing ratios were systematically ~25% too high, then the ice point is never reached. The H_2O retrieval errors are likely to be of this magnitude, although not necessarily systematic, and it is therefore possible that the measured volumes at temperatures below 189 K are the result of averaging over the FOV of sub–FOV–scale ice clouds coexisting with non–ice particles.

LTA volumes were calculated using the analytic scheme of *Carslaw et al.* [1995], and NAT volumes were calculated by assuming that HNO_3 and H_2O vapors in excess of the NAT equilibrium vapor pressures [*Hanson and Mauersberger*, 1988] are condensed onto solid particles. Although the NAT nucleation mechanism is unclear [*Tolbert*, 1996], we assume that the NAT is accompanied by sulfuric acid tetrahydrate (SAT) rather than liquid sulfuric acid. This assumption does not introduce a large error since the SAT volume is much smaller than the NAT volume. The volume calculations require the total amount of H_2SO_4 to be known. This cannot be determined directly but can be derived from the aerosol volume, water vapor pressure, and temperature, under non–PSC conditions where the aerosols are pure H_2O–H_2SO_4 (temperatures greater than about 196 K). This is possible since the droplets are in equilibrium with respect to water vapor, and H_2SO_4 in the gas phase can be neglected, as described by *Steele and Hamill* [1981]. Nitric acid was not measured during this period, and two different scenarios for nitric acid and total H_2SO_4 are now described.

4.1. Scenario 1

Aerosol volumes were calculated using the measured water vapor mixing ratios, but assuming constant HNO_3 mixing ratios of 5 and 15 ppbv and constant total H_2SO_4. For this set of calculations the total H_2SO_4 was derived from "inner vortex" measurements for temperatures between 200 and 205 K. The derived amount of 0.9 ppbv H_2SO_4 was assumed to be completely in the condensed phase. The measured aerosol volumes are compared with the calculated volumes in Figure 2. The measured volumes show increases and decreases (Figure 2b), strikingly coincident with increasing and decreasing water vapor mixing ratios (Figure 2a) at low temperatures. These volume fluctuations are very closely reproduced by the calculated LTA volumes, indicating that water strongly controls their equilibrium volume, particularly at low temperatures. In contrast, NAT growth is essentially limited by the nitric acid abundance (here assumed to be constant), and the calculated volumes are only slightly affected by changes in the water vapor. The reason for this difference is that for NAT particles, condensation of HNO_3 is essentially complete about 1 K below T_{NAT}. Changes in the abundance of water vapor below this temperature therefore have little effect on the particle growth, since

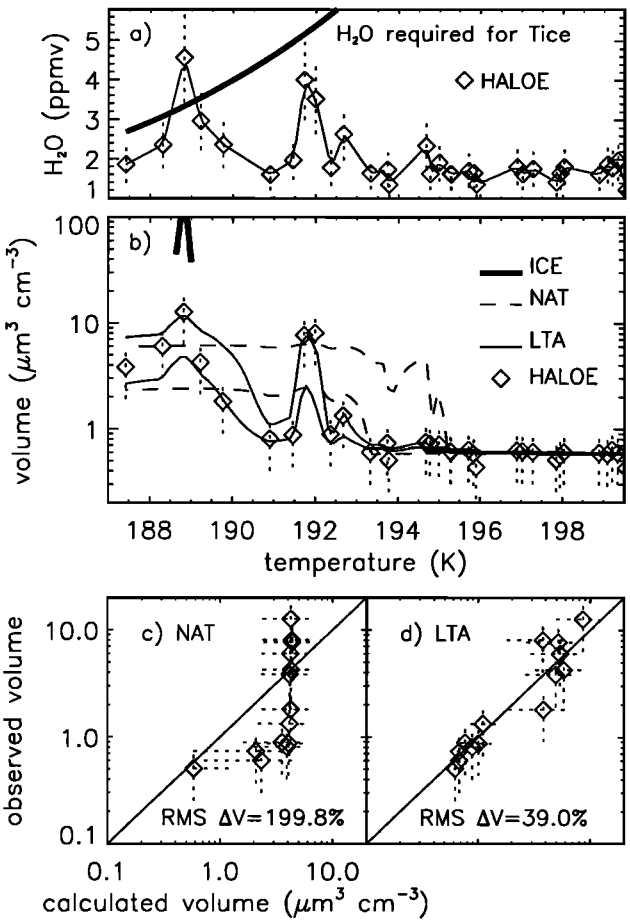

Figure 2. HALOE observations on October 7–9, 1993, at 390 K θ. Uncertainties are shown as vertical dotted lines for the measured volumes (±50%) and H_2O (±25%). (a) The measured water vapor with interpolation line and the H_2O mixing ratio required to reach the ice point. (b) The measured volumes compared with volume calculations for liquid ternary aerosols (LTA) and nitric acid trihydrate (NAT) using the measured H_2O with 5 and 15 ppbv HNO_3 (lower and upper curves) and 0.9 ppbv H_2SO_4, and ice volumes computed using the measured H_2O. Figures 2c and 2d show the correlations between observed volumes and the volumes calculated as in Figure 2b except using 10 ppbv HNO_3. Data points in Figures 2c and Figures 2d are for observations at temperatures less than 195 K, one–to–one lines are overlain, and the HALOE–model RMS volume differences for each scenario are listed. Uncertainties in measured volume are shown as vertical dotted lines. The horizontal dotted lines indicate the range of calculated volume for ±50% of the HNO_3. Note that for the lowest volumes the calculated LTA volume is relatively insensitive to the amount of HNO_3.

the stoichiometry of NAT is fixed and HNO_3 is the limiting species. For the liquid aerosols, however, the amount of H_2O absorbed into the condensed phase is variable, and changes in H_2O content affect the uptake of HNO_3 and hence the aerosol volume. These initial comparisons suggest that temperature alone would be a good predictor of NAT particle growth but a very poor predictor for liquid aerosol growth. Model calculations considering a possible ±30% systematic uncertainty in the measured water vapor (with a constant 10 ppbv HNO_3) resulted in a range of LTA volumes similar to the range obtained for 5 and 15 ppbv HNO_3 (see Figure 2b). Even when considering the possible uncertainties in measured water vapor and aerosol volume (calculations not shown), the comparison suggests that with the assumption of constant HNO_3 mixing ratios, the HALOE volumes would be consistent with LTA but not with NAT. To clarify these comparisons, Figures 2c and 2d show the observed volumes versus calculated volumes for the NAT and LTA models.

4.2. Scenario 2

In a second comparison we consider that the observed increases in water vapor could be accompanied by increases in HNO_3 and H_2SO_4. Although nitric acid measurements were not available for the period studied here, a positive correlation between H_2O and HNO_3 can be expected in the spring Antarctic vortex since both species are removed from the gas phase during PSC growth and sedimentation [*Fahey et al.*, 1989]. Microwave Limb Sounder (MLS) H_2O and HNO_3 observations [*Lahoz et al.*, 1996] from the 1992 Antarctic spring on constant pressure surfaces ranging in latitude from 50°S to 79°S on each day show a persistent positive H_2O–HNO_3 correlation. Figure 3 shows a representative comparison of H_2O and HNO_3 mixing ratios on September 9, 1992, with a linear fit overlain. Although there is a great deal of scatter, the clear correlation between H_2O and HNO_3 strongly suggests that intrusions of H_2O–rich air are likely to be associated with enhanced HNO_3. To test the effect of this on PSC growth, in the following calculations the amount of HNO_3 in an air parcel was determined from the observed water using the H_2O–HNO_3 correlation in Figure 3.

The total amount of total H_2SO_4 is also reduced within the vortex due to diabatic descent of aerosol–poor air during the winter, as indicated by the low aerosol extinctions in Plate 1. In addition, the H_2SO_4 abundance may be further reduced due to large scale gravitational sedimentation of H_2SO_4–containing particles (e.g., loss of H_2SO_4 particles contained within sedimenting ice crystals). The total H_2SO_4 should therefore increase in the intrusion region, thus contributing to the increase in aerosol volume density that is observed in the PSC. The amount of additional H_2SO_4 in the intruded air parcels cannot be determined from the aerosol volume under PSC conditions (T less than about 196 K), since the major contribution to the volume increase is the uptake of H_2O and HNO_3.

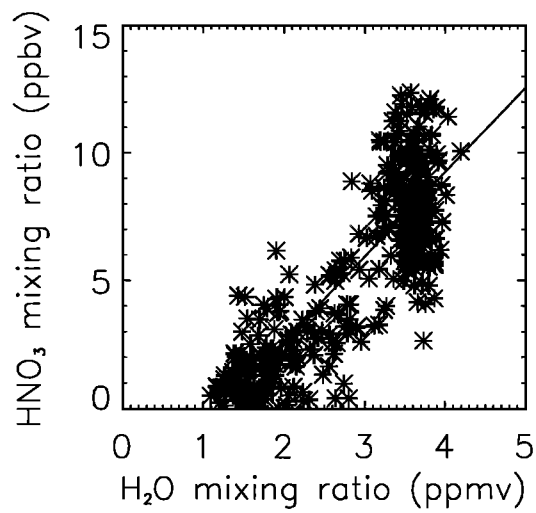

Figure 3. MLS (version 4) water vapor (Q_W) versus nitric acid (Q_N) on the 68 mbar pressure surface for measurements on September 9, 1992. The measurement latitude ranged from 50°S to 79°S, and all longitudes were used. The data were fit according to Q_N = −4.00+3.32 Q_W, for Q_W > 1.2 ppmv (solid line).

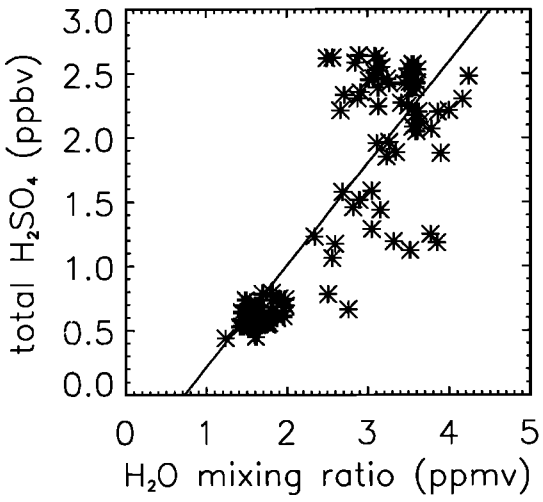

Figure 4. HALOE water vapor (Q_W) versus total H_2SO_4 (Q_S) for sunset measurements from October 4 to 9, 1993, on the 390 K θ surface. The measurement latitudes ranged from 50°S to 75°S and all longitudes were used. The data were fit according to: $Q_S = -0.61+0.81Q_W$, for $Q_W > 1$ ppmv (solid line).

To estimate the possible increase in H_2SO_4 abundance, we therefore use the correlation between total H_2SO_4 and H_2O vapor, determined under non–PSC conditions (see Figure 4). Clearly, there is a correlation between these two species, albeit weak; H_2SO_4 varies between about 2.5 ppbv for high H_2O mixing ratios outside the vortex and 0.5 ppbv for low H_2O values typical of inner vortex conditions. We use the correlation shown in Figure 4 with the observed water to determine the amount of H_2SO_4 in the following calculations. Although the uncertainty in H_2SO_4 is large (up to ±100%), the effect on calculated aerosol volume densities is relatively small (±30%), since the main contribution to aerosol growth is the uptake of H_2O and HNO_3.

The NAT and LTA volumes were recalculated using the HNO_3 and total H_2SO_4 mixing ratios determined from the measured water vapor using the correlations given in Figures 3 and 4. The resulting H_2SO_4 and HNO_3 mixing ratios are shown in Figure 5a, and the calculated and measured volumes are compared in Figure 5b. The NAT volumes are directly modulated by the nitric acid amount, resulting in volume fluctuations that are now consistent with the observations. The resulting LTA volumes are similar to the calculations using constant HNO_3 (Figure 2b) but with sharpened peaks and troughs. Changes in NAT volume due to enhanced H_2SO_4 in the intrusion air are small compared with the effects of enhanced HNO_3. Comparing the observed volumes versus calculated volumes demonstrates the drastic changes in the NAT simulations for incorporating variations in HNO_3, as the RMS HALOE–model differences are decreased from 200% to 44% (compare Figures 5c and 2c). The RMS HALOE–model volume differences for LTA decreased from 39% to 28% (compare Figures 5d and 2d). It is difficult to identify the phase of the PSC from these comparisons, however, due to the uncertainties in the mixing ratios of HNO_3 and H_2SO_4.

5. Discussion

In the preceding analysis, the inherent limitations of a large FOV were not considered. For example, observed fluctuations in water vapor could be due to the averaging of vapor–rich elements (extravortex air) and vapor–poor elements (vortex air), both within the same FOV. HALOE observations provide only an FOV–averaged H_2O signal, which, due to the nonlinear response of PSC growth to H_2O mixing ratio, cannot be used to calculated an FOV–averaged PSC volume density. However, the maximum and minimum H_2O mixing ratios are well defined, and some observations can be identified as most likely homogeneous within the FOV. Specifically, measurements of about 1.5 ppmv H_2O represent the minimum value observed over a wide area of the vortex and are therefore likely to be homogeneous on the scale of the FOV. Measurements of about 4 ppmv H_2O represent pure extravortex air, and similar arguments apply. Additionally, the limiting H_2O values observed by HALOE (about 1.5 and 4 ppmv) are consistent with other observations at different times at the same altitudes [e.g., *Fahey et al.*, 1989; *Abbas et al.*, 1996].

Similar arguments apply to the lower limit of extinction, which is bounded by the background value observed within the vortex

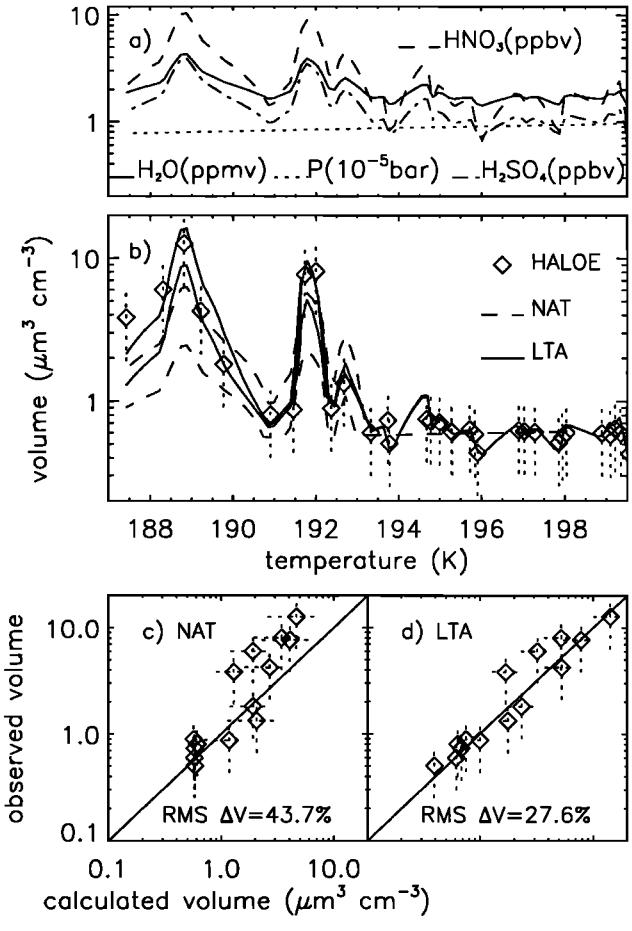

Figure 5. HALOE observations as in Figure 2. (a) The HNO_3 and total H_2SO_4 mixing ratios determined from the measured water vapor (interpolation line shown) using the relationships given in Figures 3 and 4. Pressure is also shown. (b) The measured volumes compared with volume calculations for NAT and LTA using the measured H_2O, with the H_2SO_4 in Figure 5a, and ±50% of the HNO_3 in Figure 5a (lower and upper curves). Figures 5c and 5d show the correlation between observed volumes and the volumes calculated as in Figure 5b except using the HNO_3 in panel Figure 5a. One–to–one lines are overlain and RMS HALOE–model differences are listed. Uncertainties in measured volume are shown as vertical dotted lines and the horizontal dotted lines indicate the range of calculated volume for ±50% of the HNO_3 (compare to Figures 2c and 2d).

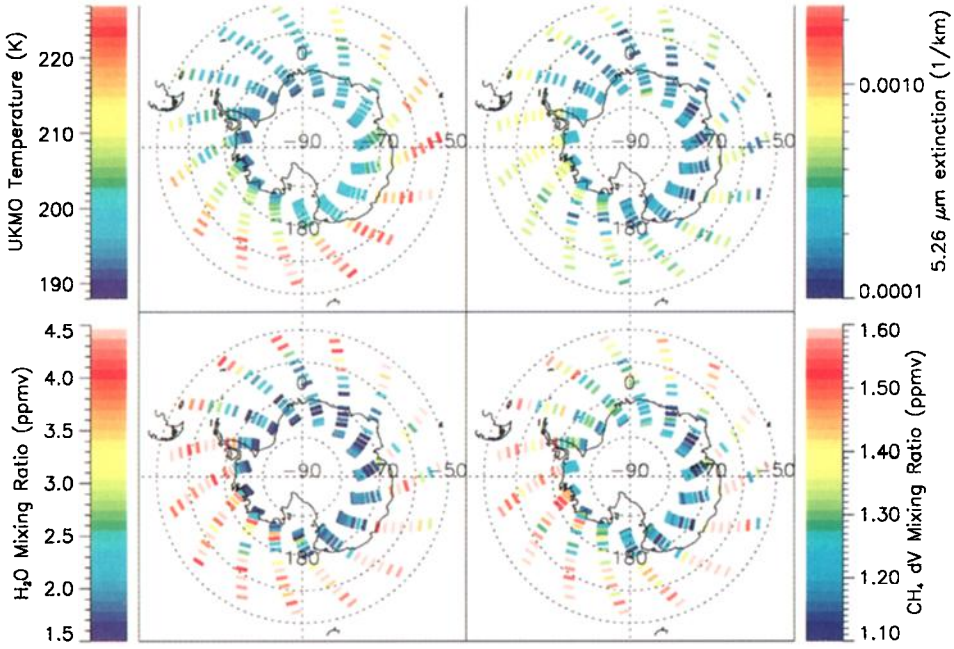

Plate 4. As in Plate 1 except the data are from October 10 (76°S) to October 25 (55°S), 1993.

(about 1×10^{-4} km^{-1}, or 0.4 μm^3 cm^{-3} in volume). An upper bound of aerosol extinction can also be identified as approximately 4×10^{-3} km^{-1} (or 10 μm^3 cm^{-3} in volume), which corresponds to near–complete removal of HNO_3 to the condensed phase by growth of either NAT or LTA PSCs (which are FOV–filling). Higher extinctions are possible for observations in ice clouds, which can reach volume densities near 100 μm^3 cm^{-3}. The possibility of ice can be excluded for observations above ~189 K; however, at lower temperatures it is possible that sub–FOV–scale ice PSCs caused an overall increase in the FOV–averaged aerosol extinction.

The large FOV causes the greatest concerns for observations of small–scale features or where strong gradients exist (such as the vortex edges). In Figures 2 and 5, the observations between the extremes are likely to fall into this category. There are justifiable arguments, however, to validate the observed maximum and minimum mixing ratios and the minimum volumes, and it is reassuring that both model and measurement have produced the same volume extremes.

6. Conclusions

HALOE observations over the eastern Weddell Sea during October 7–9, 1993, show factor of ~30 increases in aerosol volume coincident with water vapor enhancements of ~3 ppmv. The enhancement of H_2O and the coincident enhancement of HNO_3 and H_2SO_4 were considered in model calculations of PSC volume which closely match the observed volumes, suggesting that vapor resupply was an important factor in determining PSC growth. The particle type within this PSC is uncertain, however, due to uncertainties in the mixing ratios of HNO_3 and H_2SO_4.

The HALOE sunset measurements progressed northward after October 9 (75°S), reaching 50°S by October 25 (Plate 4). For this period, the HALOE water and methane fields show no evidence of enhancement, with uniformly low mixing ratios in the vortex. Although stratospheric temperatures remained low (192 K) over the Weddell Sea, there is no evidence of PSCs after October 9, which is consistent with the lack of condensible vapors. This would imply that the reformation of PSCs during October 7–9 was only temporary and that there was not an irreversible mixing of low–latitude air into the vortex.

The comparison of HALOE observations with model calculations for the growth of liquid or solid PSCs confirms the importance of the vapor distributions for the formation of late spring PSCs, as suggested by *McKenna et al.* [1989] and *Watterson and Tuck* [1989]. *Watterson and Tuck* [1989] have shown from SAM II satellite data that resupply of condensible material was important for PSC formation late in the Antarctic spring, particularly over the Weddell Sea region (longitudes from 270° to 0°E). They also observed that the incidence of PSCs diminished close to the pole even before the seasonal minimum temperatures were reached, resulting from strong dehydration and denitrification. *McKenna et al.* [1989] have also suggested that resupply of vapor from lower latitudes was important for late spring PSC formation, in a study of observations over the Weddell Sea. More specifically, our results show that the PSC volume density is strongly modulated by water vapor in the case of liquid aerosols and by nitric acid vapor in the case of NAT PSCs. The periodic resupply of vapor may lead to periods of PSC development late in the Antarctic spring, which could lead to continued heterogeneous chemistry.

Acknowledgments. We thank the HALOE science team for providing a high–quality data set, Paul Crutzen for initiating collaborations with the Max Planck Institute, and P. Newman and NCEP/CPC for providing the meteorological data. This work was supported through funding from the NASA Langley Research Center.

References

Abbas, M. M., et al., Seasonal variations of water vapor in the lower stratosphere inferred from ATMOS/ATLAS 3 measurements of H_2O and CH_4, *Geophys. Res. Lett.*, *23*, 2401–2404, 1996.

Adriani, A., T. Deshler, G. Di Donfrancesco, and G. P. Gobbi, Polar

stratospheric clouds and volcanic aerosol during spring 1992 over McMurdo Station, Antarctica: Lidar and particle counter comparisons, *J. Geophys. Res., 100,* 25,877–25,897, 1995.

Boone, T. L., K. A. Fuller, and H. D. Downing, Infrared optical constants of aqueous solutions of nitric acid, *J. Phys. Chem., 84,* 2666–2667, 1980.

Carslaw, K. S., B. P. Luo, S. L. Clegg, Th. Peter, P. Brimblecombe, and P. J. Crutzen, Stratospheric aerosol growth and gas phase denitrification from nitric acid and water uptake by liquid particles, *Geophys. Res. Lett., 21,* 2479–2482, 1994.

Carslaw, K. S., B. P. Luo, and Th. Peter, An analytic expression for the composition of aqueous HNO_3–H_2SO_4 stratospheric aerosols including gas phase removal of HNO_3, *Geophys. Res. Lett., 22,* 1877–1880, 1995.

Carslaw, K.S., Th. Peter, and S.L. Clegg, Modeling the composition of liquid stratospheric aerosols, *Revs. Geophys., 35,* 125–154, 1997.

Deshler, T., B. J. Johnson, and W. R. Rozier, Changes in the character of polar stratospheric clouds over Antarctica in 1992 due to the Pinatubo volcanic aerosol, *Geophys. Res. Lett., 21,* 273–276, 1994.

Drdla A., A. Tabazadeh, R. P. Turco, M. Z. Jacobsen, J. E. Dye, C. Twohy, and D. Baumgardner, Analysis of the physical state of one Arctic polar stratospheric cloud based on observations, *Geophys. Res. Lett., 21,* 2475–2478, 1994.

Dye, J. E., D. Baumgardner, B. W. Gandrud, S. R. Kawa, K. K. Kelly, M. Lowenstein, G. V. Ferry, K. R. Chan, and B. L. Gary, Particle size distributions in Arctic polar stratospheric clouds, growth and freezing of sulfuric acid droplets, and implications for cloud formation, *J. Geophys. Res., 97,* 8015–8035, 1992.

Fahey, D. W., D. M. Murphy, K. K. Kelly, M. K. W. Ko, M. H. Proffitt, C. S. Eubank, G. V. Ferry, M. Loewenstein, and K. R. Chan, Measurements of nitric oxide and total reactive nitrogen in the Antarctic stratosphere: Observations and chemical implications, *J. Geophys. Res., 94,* 16,665–16,681, 1989.

Hanson, D., and K. Mauersberger, Laboratory studies of the nitric acid trihydrate: Implications for the south polar stratosphere, *Geophys. Res. Lett., 15,* 855–858, 1988.

Harries, J. E., J. M. Russell III, A. F. Tuck, L. L. Gordley, P. Purcell, K. Stone, R. M. Bevilacqua, M. Gunson, G. Nedoluha, and W. Traub, Validation of measurements of water vapour from the Halogen Occultation Experiment (HALOE), *J. Geophys. Res., 101,* 10,205–10,216, 1996.

Hartmann, D. L., and L. E. Heidt, Transport into the south polar vortex in early spring, *J. Geophys. Res., 94,* 16,779–16,795, 1989.

Hervig, M. E., J. M. Russell III, L. L. Gordley, J. Daniels, S. R. Drayson, and J. H. Park, Aerosol effects and corrections in the Halogen Occultation Experiment, *J. Geophys. Res., 100,* 1067–1079, 1995.

Hervig, M. E., J. M. Russell III, L. L. Gordley, J. H. Park, and S. R. Drayson, and T. Deshler, Validation of aerosol measurements from the Halogen Occultation Experiment, *J. Geophys. Res., 101,* 10,267–10,275, 1996a.

Hervig, M. E., et al., Validation of temperature measurements from the Halogen Occultation Experiment, *J. Geophys. Res., 101,* 10,277–10,285, 1996b.

Hofmann, D. J., and T. Deshler, Stratospheric cloud observations during the formation of the Antarctic ozone hole in 1989, *J. Geophys. Res., 96,* 2897–2912, 1991.

Koop, T., B. Luo, U. M. Biermann, P. J. Crutzen, and Th. Peter, Freezing of HNO_3 /H_2SO_4 /H_2O solutions at stratospheric temperatures: nucleation statistics and experiments, *J. Phys. Chem., 101,* 1117–1133, 1995.

Koop, T., K. S. Carslaw, and Th. Peter, Thermodynamic stability and phase transitions of polar stratospheric cloud particles, *Geophys. Res. Lett., 24,* 2199–2202, 1997.

Luo, B. P., U. K. Krieger, and Th. Peter, Densities and refractive indices of H_2SO_4 /HNO_3 /H_2O solutions to stratospheric temperatures, *Geophys. Res. Lett., 23,* 3707–3710, 1997.

Lahoz, W. A., et al., Validation of UARS Microwave Limb Sounder 183–GHz H_2O measurements, *J. Geophys. Res., 101,* 10,129–10,149, 1996.

Manney, G. L., R. Swinbank, S. T. Massie, M. E. Gelman, A. J. Miller, R. Nagatani, A. O'Niell, and R. W. Zurek, Comparison of U.K. Meteorological Office and U.S. National Meteorological Center stratospheric analyses during northern and southern winter, *J. Geophys. Res., 101,* 10,311–10,334, 1996.

McKenna, D. S., R. L. Jones, and J. Austin, Diagnostic studies of the Antarctic vortex during the 1987 airborne Antarctic Ozone Experiment: Ozone miniholes, *J. Geophys. Res., 94,* 11,641–11,641, 1989.

Molina, M. J., R. Zhang, P. J. Woolridge, J. R. McMahon, J. E. Kim, H. Y. Chang, and K. D. Beyer, Physical chemistry of the H_2SO_4 /H_2O /HNO_3 system: Implications for polar stratospheric clouds, *Science, 261,* 1418–1423, 1993.

Murphy, D. M., A. F. Tuck, K. K. Kelly, K. R. Chan, M. Loewenstein, J. R. Podolske, M. H. Proffitt, and S. R. Strahan, Indicators of transport and vertical motion from correlations between in situ measurements in the Airborne Antarctic Ozone Experiment, *J. Geophys. Res., 94,* 11,669–11,685, 1989.

Palmer, K. F., and D. Williams, Optical constants of sulfuric acid: Application to the clouds of Venus?, *Appl. Opt., 14,* 208–219, 1975.

Peter, Th., The microphysics and chemistry of polar stratospheric cloud particles, *Ann. Rev. Phys. Chem.*, in press, 1997.

Russell, J. M., III, L. L. Gordley, J. H. Park, S. R. Drayson, W. D. Hesketh, R. J. Cicerone, A. F. Tuck, J. E. Frederick, J. E. Harries, and P. J. Crutzen, The Halogen Occultation Experiment, *J. Geophys. Res., 98,* 10,777–10,797, 1993a.

Russell, J. M., III, A. F. Tuck, L. L. Gordley, J. H. Park, S. R. Drayson, J. E. Harries, R. J. Cicerone, and P. J. Crutzen, HALOE Antarctic observations in the spring of 1991, *Geophys. Res. Lett., 20,* 719–722, 1993b.

Steele, H. M., and P. Hamill, Effects of temperature and humidity on the growth and optical properties of sulfuric acid–water droplets in the stratosphere, *J. Aerosol Sci., 12,* 517–528, 1981.

Tabazadeh, A., and O. B. Toon, The presence of metastable HNO_3/H_2O solid phases in the stratosphere inferred from ER 2 data, *J. Geophys. Res., 101,* 9071–9078, 1996.

Tabazadeh, A., R. P. Turco, K. Drdla, and M. Z. Jacobson, A study of type I polar stratospheric cloud formation, *Geophys. Res. Lett., 21,* 1619–1622, 1994.

Tolbert, M. A., Polar clouds and sulfate aerosols, *Science, 272,* 1597, 1996.

Toon, O. B., M. A. Tolbert, B. G. Koehler, A. M. Middlebrook, and J. Jordan, Infrared optical constants of H_2O ice, amorphous nitric acid solutions, and nitric acid hydrates, *J. Geophys. Res., 99,* 25,631–25,645, 1994.

Watterson, I. G., and A. F. Tuck, A comparison of the longitudinal distributions of polar stratospheric clouds and temperatures for the 1987 Antarctic spring, *J. Geophys. Res., 94,* 16,511–16,525, 1989.

K. S. Carslaw and T. Peter, Max–Planck–Institut für Chemie, Postfach 3060, D–55020 Mainz, Germany. (email: carslaw@nike.mpch–mainz.mpg.de)

T. Deshler and M. E. Hervig, Department of Atmospheric Science, University of Wyoming, P.O. Box 3038, Laramie, WY 82071. (email: hervig@trex.uwyo.edu)

L. L. Gordley, GATS Inc., 28 Research Dr., Hampton, VA 23666. (email: larry@gatsibm.larc.nasa.gov)

G. Redaelli, Dipartimento di Fisica, Univ. degli Studi, L'Aquila, Italy. (email: redaelli@axscaq.aquila.infn.it)

J. M. Russell III, Center for Atmospheric Sciences, Hampton University, Hampton, VA 23681. (email: jmr@hamptonu.edu)

(Received September 6, 1996; revised August 21, 1997; accepted August 27, 1997.)